Hindawi
Mathematical Problems in Engineering
Volume 2023, Article ID 8702719, 12 pages
https://doi.org/10.1155/2023/8702719

Research Article

Failure Analysis of Tubing Collapse in a Gas Well

Jinlan Zhao[1], **Ke Tong**[1], **Junjie Lei**[2], **Xiaoliang Bai**[1], **Dongfeng Li**[1], **Zhaoxi Shen**[1], **Tingting Qu**[1], and **Xiaolong Li**[1]

[1] *Tubular Goods Research Center of CNPC, Key Laboratory of Petroleum Tubular Goods and Equipment Quality Safety for State Market Regulation, Xi'an, Shaanxi 710077, China*
[2] *Xi'an Institute of Applied Optics, Xi'an, Shaanxi 710065, China*

Correspondence should be addressed to Jinlan Zhao; 147665020@qq.com

Received 19 October 2022; Revised 8 May 2023; Accepted 11 May 2023; Published 1 December 2023

Academic Editor: Rafael Morales

The tubing used in a gas well rarely collapses and fails during applying annulus pressure. In this study, the failure causes of tubing collapse were analyzed by means of data verification, macroscopic observation, magnetic particle inspection, physical and chemical inspection, optical microscopy, and tubing collapse test. Mechanical analysis of the string and full-scale physical simulation test simulating downhole working conditions. Finally, the verification analysis of the collapse test is carried out by the finite element analysis (FEA). The results showed that (1) the physical dimension, physical and chemical properties, and collapse resistance of this batch of tubing met the requirements of the tubing ordering technical standard. (2) Assuming that the well packer slip was unsealed and could slide freely, the mechanical theoretical analysis of collapsed tubing string and collapse test under simulated working condition load was carried out, which reproduced the load when the tubing collapsed. It can be seen from this that the packer did fail. (3) The FEA calculation results showed that when the external pressure was greater than 30.75 MPa, it would inevitably lead to collapse failure in case of packer unsealed. In conclusion, the root cause for the collapse failure of the 105th underground tubing string was that the packer lost its sealing function, resulting in an abnormal axial load. While under the action of external pressure, the tubing was overloaded and collapsed. It is recommended to carry out verification tests on the material performance of packer slip, the dimensional changes of packer tool outer diameter and inner diameter under actual well conditions, the creep behavior of packer seal, and the performance of shear pin under actual working conditions, especially in the well containing H_2S, so as to prevent the pressure leakage of gas well annulus caused by packer unsealing and the reoccurrence of such downhole string collapse accidents. The first collapse test under simulated working condition load is conducted in this paper. Analyzing the collapse failure work and putting forward suggestions to effectively prevent similar failures from happening again are of great significance to the oilfield.

1. Introduction

With the increase in the number of complex drilling operations, such as deep and ultra-deep wells, the load on the casing string has become increasingly complex, and oil fields are paying increasing attention to wellbore integrity management. According to the research of Zhang et al. [1], Dethlefs and Chastain [2], Samuel [3], and Singh et al. [4], once the integrity of the wellbore is damaged or fails, the highly corrosive and toxic hydrogen sulfide may leak seriously, which not only causes huge economic losses but also seriously endangers the environment and public life safety. Therefore, drilling and string safety production are issues that the world's oil and gas fields need to jointly face and solve.

For the integrity of the wellbore, domestic and foreign scholars have mainly made the research work of the following aspects.

1.1. Buckling Behavior. We followed the research of Dethlefs and Chastain [2] and Samuel [3]; the integrity of the wellbore is closely related to the integrity of the oil casing string. Singh et al. [4] proposed that the rationality of the pipe string structure was a key factor affecting the safety and reliability of the casing string. In recent years, Mitchell [5, 6] and

Lubinski [7] have conducted extensive research on the mechanics of the completion string, indicating that the buckling behavior of the downhole oil casing string and the optimization design of the string were crucial. Shokry and Elgibaly [8] developed a well design optimization through the elimination of intermediate casing string. Mohammed et al. [9] investigated the structural integrity of casing under radial and axial configurations using two simulation scenarios. Zhang et al. [10] proposed a new model to describe the buckling morphology of a pipe string in a 3D curved wellbore. Using this model, it can guide the selection of control parameters for on-site pipe columns. Tan and Digby [11] researched the buckling of drill strings under the action of gravity and axial thrust. We followed the research of Mohammed et al. [12], which introduced the main causes of casing failure in different well types and the classification of cases and identified the existing tools used to evaluate well integrity issues and their respective limitations.

1.2. Abnormal Pressure. The rationality of the string structure can effectively ensure the safety of the pipe column and prevent failure caused by annular pressure leakage. In recent years, domestic and foreign scholars have conducted theoretical research on the abnormal pressure of gas well annulus and packers in response to complex downhole usage conditions. Liao et al. [13] proposed a transient gas–liquid–solid multiphase flow model for gas surge during managed pressure drilling operations and considering the effect of dynamic wellhead back-pressure, temperature field, and velocity relation of different phases. Qian-bei et al. [14] studied an approach to assess the mechanical properties of a packer in multistage fracturing technology with immovable string.

1.3. Yield Strength. Deng et al. [15] proposed a new high collapse model to predict the collapse strength based on the unified strength theory. Taheri et al. [16] analyzed rock salt layer creep and its effects on casing collapse based on extensive experiments. Guo et al. [17] developed a safety evaluation method for high-pressure, high-temperature, and high-yield gas well tubing, providing a theoretical method for the safety evaluation of complex gas well tubing.

The above studies principally focused on the buckling behavior of downhole oil casing string, the rationality of string structure, the optimal design of string, the calculation and prediction of casing collapse strength, abnormal pressure in gas well annulus based on the model, performance evaluations for packers in multistage fracturing technology with immobile strings. However, there are few studies on the tubing collapse failure, mostly about the casing collapse in a well. Few studies on tubing collapse are limited to theoretical methods for the safety evaluation of tubing string. Nevertheless, tubing collapse accidents from abnormal annular pressure caused by packer failure in the downhole cannot be ignored, and research in this area is highly significant for specification operation and preventing the recurrence of such accidents.

This article introduces the situation that a tubing collapse occurred in a gas well in western China, causing the tubing string to fall into the well. When the annulus of the fracturing truck was pressurized to 42.5 MPa, a muffled sound was heard on the ground, and there was an obvious vibration at the choke and kill manifold. Then, the casing pressure drop was 0 MPa. The subsequent inspection found that the 105th tubing located 999.16 m underground collapsed. The specification of the collapsed tubing is Φ88.9 mm × 6.45 mm 110SS, and the ordering technical standard is API Spec 5CT-2018 and additional technical agreement. Figure 1 shows the morphology of the failed sample.

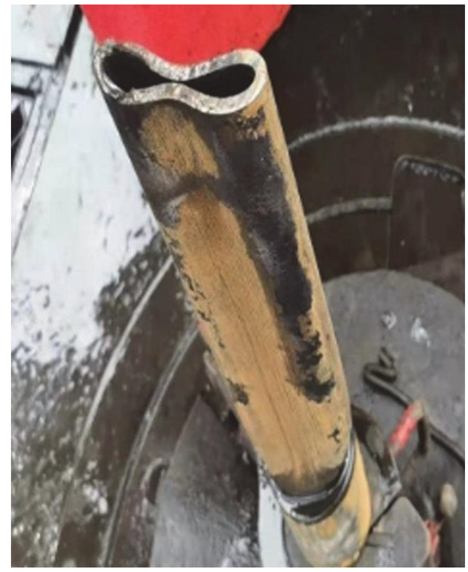

Figure 1: Morphology of the collapsed tubing.

In order to find the failure reason for the collapsed tubing, data verification, macroscopic observation, magnetic particle inspection, physical and chemical inspection, optical microscopy, and collapse strength inspection were carried out. The comprehensive analysis, including theoretical calculation and analysis on mechanics of collapsing tubing string, reproduction of collapse test simulating downhole load conditions, and the finite element analysis (FEA) of a partial model of the gas well tubing string, was used to analyze the pipe string mechanics. Finally, the reason for the collapse failure was analyzed, and relevant suggestions were proposed to prevent such accidents from occurring.

2. Materials and Methods

The surface of the failed tubing body and the same batch of tubing body that had not failed were examined by magnetic particle inspection using the LKNB-22016UV magnetic particle flaw detector according to NB/T 47013.4-2015 standards. The chemical composition of the tubing was analyzed using ARL 4460 direct reading spectroscopy according to ASTM A751-20 standards. The plate tensile sample with a gauge of 50 mm × 19.1 mm was cut longitudinally along the tubing. The SHT4106 testing machine was used to test the tensile properties of the tubing samples according to ASTM A370-20 standards. Impact specimens were cut longitudinally along the tubing and machined into 5 mm × 10 mm × 55 mm Charpy V-notch impact specimens. The Charpy impact

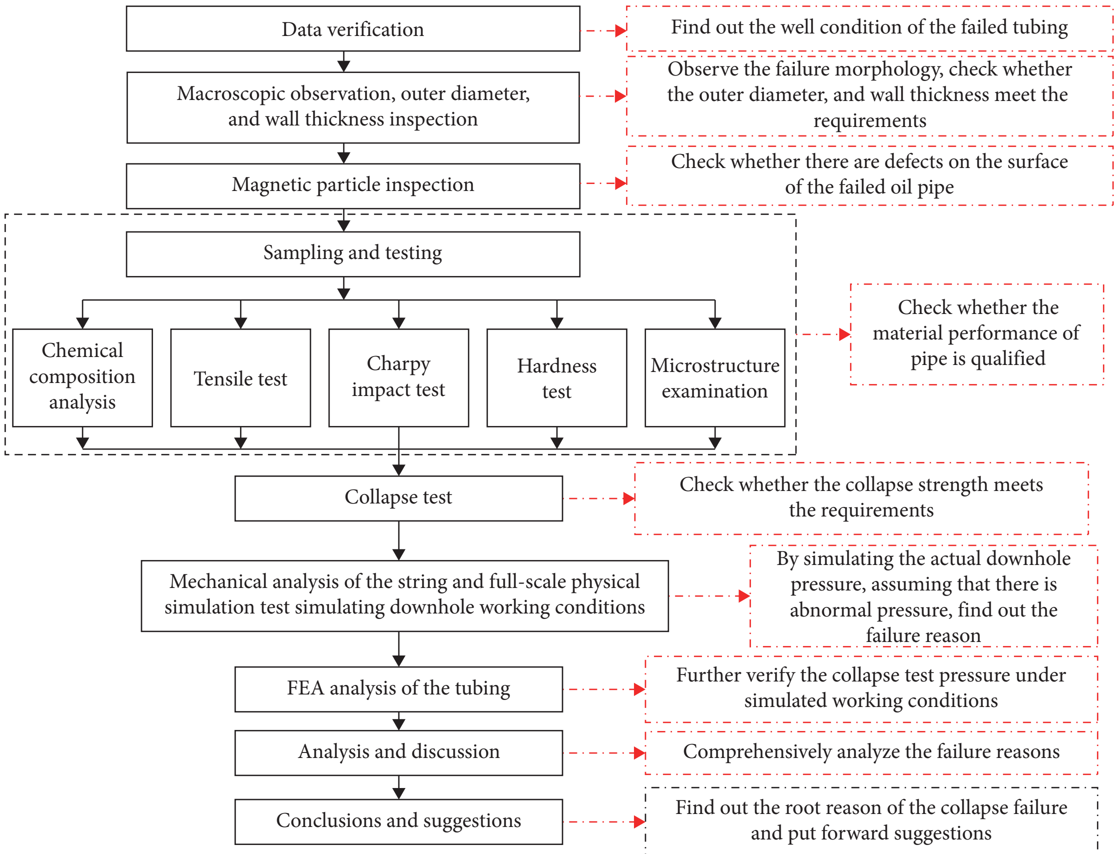

FIGURE 2: Workflow of this failure analysis.

energy of the failed samples was measured on a JB-800 impact tester at 0°C in accordance with ASTM A370-20, and the average of the results of three impacts at each temperature was taken. The Rockwell hardness test of the tubing was analyzed using RB2002T Rockwell hardness tester according to ASTM E18-20 standards. The microstructure, grain size, and nonmetallic inclusions of the tubing were analyzed using a MEF3A metallographic microscope and an OLS 4100 laser confocal microscope according to ASTM E3-11 (2017), ASTM E45-18a and ASTM E112-13 standards.

According to ISO/TR 10400-2018, a collapse test was conducted on the same batch of tubing used by the same manufacturer.

According to ISO/TR 10400-2018, the loads of the failed tubing in service in case of collapse failure were analyzed and calculated. Further, assume that the packer fails, so as to calculate the abnormal axial load on the failed tubing. Finally, the simulation test of collapse test under abnormal axial load was carried out in the laboratory.

In order to find out the root reason of the collapse failure, a failure analysis test and detection scheme are developed (see data in Figure 2).

3. Results

3.1. Data Verification. The gas well is a highly deviated well with a completed drilling depth of 6,133.00 m (vertical depth of 5,559.15 m). The H_2S content is 14.07 g/m^3, the formation pressure coefficient is 1.10, the estimated formation pressure is 59.98 MPa, and the maximum shut-in pressure of the wellhead when it is pure natural gas is expected to be 45.68 MPa. The bottom hole temperature is 173.7°C. Figure 3 shows the schematic diagram of the well structure. The collapsed tubing is located at the well depth of 999.16 m and is the first tubing under the variable thread joint. The specification of the tubing here is changed from Φ88.9 mm × 9.53 mm 110SS special thread tubing to Φ88.9 mm × 6.45 mm 110SS special thread tubing.

3.2. Macroscopic Observation. The collapsed tubing was severely deformed, flat, yellowish brown on the surface, and rusted. From the both ends of the collapsed tubing, the cross-section of the tubing was in the shape of "8." In order to master the internal situation of the failed tubing, cut the collapsed tubing along the two ends of the extruded flattened tubing (Figure 4), and there was no blocking foreign matter on the inner wall of the collapsed tubing.

3.3. Outer Diameter and Wall Thickness Inspection. MMX-6DL ultrasonic thickness gauge was used to measure the wall thickness of the failed tubing along the longitudinal direction of the tubing body. The results showed that due to extrusion deformation, the wall thickness of the failed tubing body was small on the side of the "8" outer arc side, and the wall thickness near the "8" central groove was large. The minimum wall thickness after extrusion deformation is 5.87 mm,

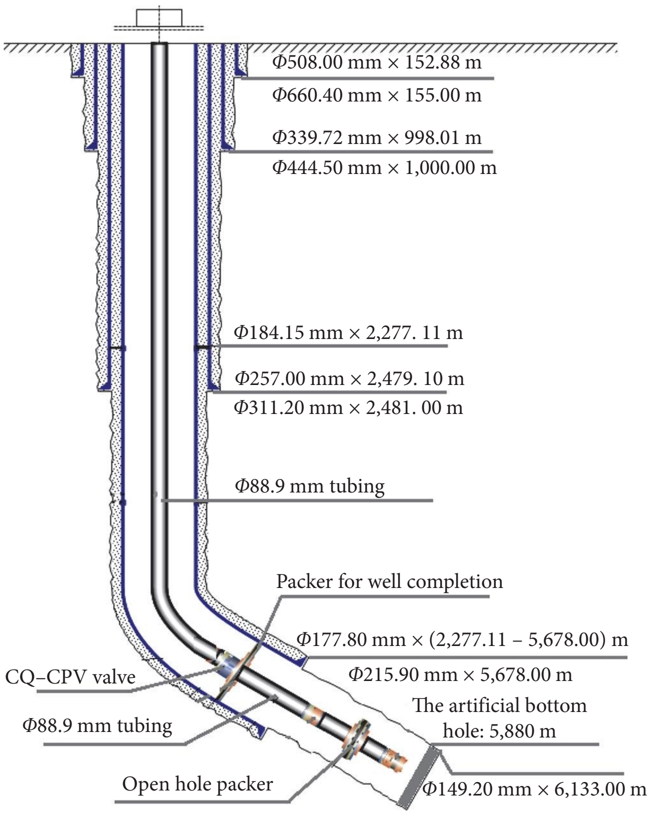

FIGURE 3: Schematic diagram of wellbore structure.

FIGURE 4: Macromorphology of cross-section of failed tubing.

which is in line with the requirements of the order technology (≥5.64 mm).

The wall thickness and outer diameter of the same batch of used tubing without failure were measured. The measurement position is the longitudinal section of the tubing body, and the spacing of each section is 200 mm. The wall thickness of each section is measured at eight positions in the circumferential direction (0°, 45°, 90° 135°, 180°, 225°, 270°, and 315°). Figure 5 shows the measurement distribution diagram. The results showed that the outer diameter and wall thickness of the same batch of tubing were in line with the requirements of the order technology.

3.4. Magnetic Particle Inspection. According to NB/T 47013.4-2015, magnetic particle inspection was carried out on the outer surface of failed tubing and the same batch of tubing that had not failed. Table 1 shows the test conditions of magnetic particle inspection. The results show that there were no cracks on the outer surface of the tubings.

3.5. Physical and Chemical Tests. According to ASTM a751-14a, the chemical composition of failed tubing and the same batch of tubing that had not failed were analyzed. Table 2 shows the results of the magnetic particle inspection. The results showed that the chemical composition of this batch of tubings was in line with the requirements of the order technology.

According to ASTM A370-20, the tensile properties, Charpy impact properties, and hardness properties of failed tubing and the same batch of tubing that had not failed were carried out. Tables 3 and 4 show the results of tensile and Charpy impact. The results showed that the yield strength of failed tubing increased due to deformation hardening. The mechanical properties of the same batch of tubing bodies met the requirements of the order technology.

According to ASTM E3-11 (2017), ASTM E45-13, and ASTM E112-13, the microstructure, grain size, and inclusions of failed tubing and the same batch of tubing that had not failed were analyzed. Table 5 and Figure 6 show the results of the microstructure, grain size, and inclusions. The analysis results showed that the metallographic structure of the tubing body was tempered sorbite, the grain size was grade 9.5, and the nonmetallic inclusions in the tubing body were very small. The results showed that there was no abnormal microstructure in the failed tubing.

3.6. Collapse Test. According to ISO/TR 10400-2018, a collapse test was conducted on the same batch of tubing used by the same manufacturer. Table 6 and Figure 7 show the results of the collapse test. The test results showed that the collapse strength met the requirements of ordering technical agreement requirement.

4. Mechanical Analysis of the String and Full-Scale Physical Simulation Test Simulating Downhole Working Conditions

According to the comprehensive performance test results of the failed tubing and the same batch of tubing, the wall thickness, outer diameter, physical and chemical properties, and collapse resistance of this batch of tubing are in line with the requirements of the order technology. Therefore, it can be seen that collapse failure will not occur if the tubing bearing is subjected to normal service load because the collapse strength of the tubing is in line with the requirements of the order technology.

In order to find the failure reason for the collapsed tubing, the mechanical analysis of the string was carried out, and the full-scale physical simulation test simulating downhole working conditions was carried out according to the stress condition of the collapsed tubing to determine the root cause of this collapse failure.

4.1. Analysis of the Loads of the Failed Tubing in Service in Case of Collapse Failure. According to ISO/TR 10400-2018, the loads of the failed tubing in service in case of collapse failure were analyzed and calculated.

4.1.1. External Loads of the 105th Tubing in Case of Collapse Failure. According to the well condition data, the external loads on the 105th tubing at the moment of failure were calculated as follows:

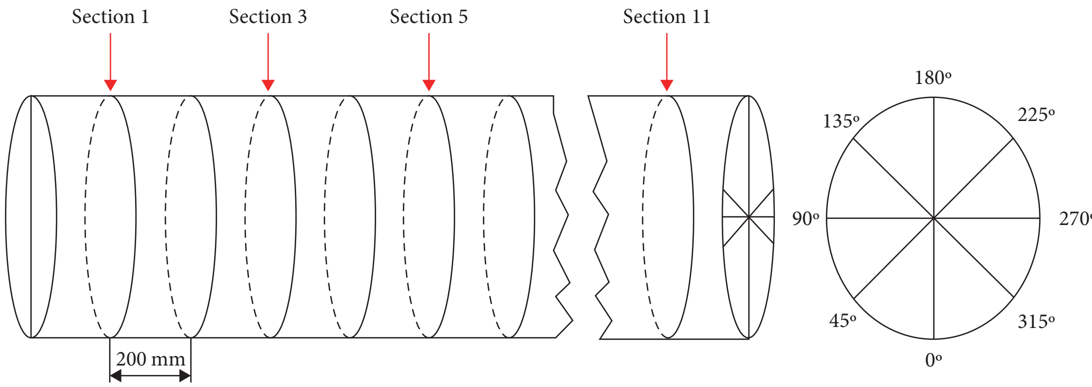

Figure 5: Schematic diagram of geometric dimension measurement of tubing body used in the same batch.

Table 1: The conditions of magnetic particle inspection.

Equipment	Magnetization specification	Magnetic particle type	Inspection method	Magnetization method	Test location
Y-1	Lifting power ≥45 N	Fluorescent magnetic particle	Wet continuous method	Yoke magnetizing method	External surface of pipes

Table 2: Chemical composition of failed tubing and the same batch of tubing without failure (wt.%).

Element Sample	C	Si	Mn	P	S	Cr	Mo
Failed pipe body	0.19	0.19	0.48	0.0063	0.0011	0.49	0.72
The tubing body in the same batch	0.19	0.19	0.48	0.0057	0.001	0.50	0.73
Requirements of ordering technical agreement requirement	≤0.35	≤0.50	≤1.20	≤0.015	≤0.003	0.10–1.60	0.20–1.20

Table 3: Mechanical properties of the failed tubing and the same batch of tubing without failure.

Sample	Tensile test			Charpy impact test
	R_m (MPa)	$R_{t0.7}$ (MPa)	A (%)	KV_2 (J)
Failed pipe body	906	851	15	89, 97, 95
The tubing body in the same batch	833	791	22	117, 119, 116
Requirements of ordering technical agreement requirement	≥793	758–828	≥12	≥44 29≤ Only allow 1 value <44

$$P_0 = P_{01} + \rho g h_1 / 1{,}000, \tag{1}$$

where P_0 is the external loads on the 105th tubing at the moment of collapse failure (MPa); P_{01} is the external pressure of the wellhead (42.45 MPa); ρ_1 is the density of displacing fluid (1.0 kg/m); g is the gravitational acceleration (9.8 N/kg); h_1 is the depth of the 105th tubing in the well (999.16 + 10 m).

So, $P_0 = 42.45 + 1.0 \times 9.8 \times (999.16 + 10)/1000 = 52.33$ MPa. That is, when the 105th tubing collapsed, the external pressure was 52.3 MPa, which was far lower than the required value of collapse strength (93.3 MPa) and the collapse strength test value of 4# same batch of tubing (94.5 MPa).

Therefore, it can be inferred that when the 105th tubing collapsed, it should also be subjected to abnormal axial load on the basis of 52.3 MPa external pressure.

4.1.2. Analysis of the Axial Load on the 105th Tubing in Case of Collapse Failure. The abnormal axial load comes from the complex stress condition of the tubing downhole. One of the abnormal axial loads was analyzed as below.

According to the field data, the drilling crew used two 700 fracturing trucks to control pressure and reverse and replace 125.0 m^3 of clean water, including 100.0 m^3 of clean water and 25.0 m^3 of well-washing fluid. A 700 fracturing truck was used to slowly pressurize the tubing with clean water. The pressure of the tubing changed from 11.37 to 37.12 MPa, then decreased to 35.09 MPa, and finally increased to 38.14 MPa. The casing pressure increased from 3.58 to 5.26 MPa. After 30 min of pressure stabilization, the packer setting was completed.

Assuming that the temperature decreased due to liquid displacement before setting, the string shrinked. After the

Table 4: Hardness test of the failed tubing and the same batch of tubing without failure.

Sample		Hardness test (HRC)															
		Quadrant I				Quadrant II				Quadrant III				Quadrant IV			
		Single value			Average value	Single value			Average value	Single value			Average value	Single value			Average value
Failed pipe body	Outer surface	27.3	27.7	27.6	27.5	27.6	27.4	27.3	27.2	26.0	27.2	27.1	26.8	26.9	27.2	27.1	27.1
	Center	27.8	27.7	27.8	27.8	26.4	27.6	27.5	27.4	27.6	27.7	27.6	27.6	27.2	27.3	27.3	27.3
	Inner surface	27.5	27.8	27.5	27.6	27.8	27.7	27.4	27.6	27.8	27.7	27.6	27.7	27.2	27.5	27.5	27.4
Variation value		0.3				0.4				0.9				0.2			
The tubing body in the same batch	Outer surface	25.9	25.7	25.8	25.8	25.4	25.6	26.2	25.7	24.9	25.9	25.5	25.4	25.7	24.9	24.9	25.2
	Center	25.4	26.0	25.7	25.7	25.8	26.3	25.9	26.0	26.3	25.8	26.3	26.1	25.9	26.3	26.3	26.2
	Inner surface	25.4	25.4	25.9	25.6	25.6	23.8	25.4	24.9	25.4	25.3	25.8	25.5	25.9	26.1	26.1	26.0
Variation value		0.2				1.1				0.7				1.0			
Requirements of ordering technical agreement requirement		Single value ≤28.5 Variation value ≤3.0															

Table 5: Microstructure examination results of the failed tubing and the same batch of tubing without failure.

Sample position	Nonmetallic inclusions								Microstructure	ASTM grain size
	A		B		C		D			
	Thin	Thick	Thin	Thick	Thin	Thick	Thin	Thick		
Failed pipe body	0.5	0	0.5	0	0	0	1.0	0	Tempered sorbite (Figure 5)	9.5
The tubing body in the same batch	0.5	0	0.5	0	0	0	1.0	0	Tempered sorbite (Figure 5)	9.5

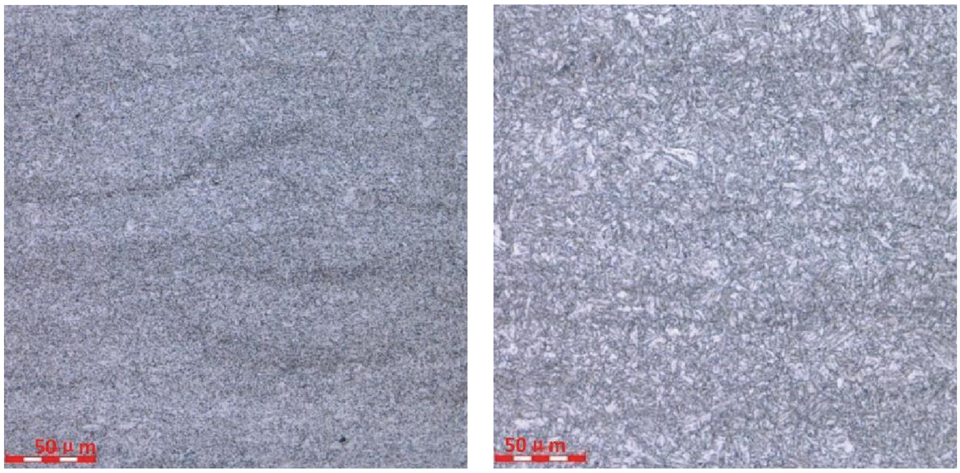

(a) (b)

Figure 6: Metallographic structure of the tubings: (a) metallographic structure of the failed pipe body; (b) metallographic structure of the pipe body in the same batch.

Table 6: Collapse test results of the same batch of tubing without failure.

Sample	External load (MPa)	Result
The tubing without failure in the same batch	94.5	The tubing body was collapsed and failed
Requirements of ordering technical agreement requirement	≥93.3	—

Figure 7: The morphology of the same batch of tubing after collapse test.

Table 7: Stress load comparison results of simulated collapse test and failed tubing in the well.

Sample	Axial load (kN)	External pressure (MPa)	Results	Remarks
The same batch of tubing	1,146	52.5	The pipe body was collapsed	There are slight differences in the performance of the same batch of tubing, which can be ignored
Failed tubing in the well	1,146	52.3	The pipe body was collapsed	

packer was set, the string was elongated again, which caused the tensile load decreased. If the packer slip failed, the packer would slide freely, and the setting internal pressure and temperature load would disappear. Therefore, these two effects would be ignored.

(1) Calculation of string weight tension generated at 999.16 m depth of accident well

The string weight tension generated at a depth of 999.16 m was calculated as follows:

$$G = \rho_2 g h_2 / 1{,}000, \tag{2}$$

where G is the string weight tension generated at a depth of 999.16 m (kN); ρ_2 is the density of the pipeline (13.42 kg/m); g is the gravitational acceleration (9.8 N/kg); h_2 is the string length below failed string ((5,822–999.16) m).

So,

$$G = 13.42 \times 9.8 \times (5{,}822 - 999.16)/1{,}000 = 634.28\,\text{kN}. \tag{3}$$

(2) Calculation of tensile force assuming packer slip failed

(i) The internal pressure of the packer was calculated as follows:

$$P_{i0} = P_{i1} + \rho_1 g h_3/1{,}000, \tag{4}$$

where P_{i0} is the internal pressure of the packer assuming that the packer slip failed (MPa); P_{i1} is the pressure in the wellhead pipe (0 MPa); ρ_1 is the density of clean water in the tubing (1.0 kg/m); g is the gravitational acceleration (9.8 N/kg); h_3 is the height of packer in this well (5,408 m).

So,

$$P_{i0} = 0 + 1.0\times 9.8\times 5{,}408/1{,}000 = 53.05\,\text{MPa}. \tag{5}$$

(ii) The external pressure of the packer was calculated as follows:

$$P_{02} = P_{01} + \rho_1 g h_3/1{,}000, \tag{6}$$

where P_{02} is the external pressure of the packer assuming that the packer slip failed (MPa); P_{01} is the external pressure of the wellhead pipe (42.45 MPa); ρ_1 is the density of clean water in the tubing (1.0 kg/m); g is the gravitational acceleration (9.8 N/kg); h_3 is the height of packer in this well (5,408 m).

So,

$$P_{02} = 42.45 + 1.0\times 9.8\times 5{,}408/1{,}000 = 95.50\,\text{MPa}. \tag{7}$$

(iii) The failed tubing is Φ88.9 mm × 6.45 mm 110SS, and the outer casing of failed tubing is Φ184.15 mm × 15.83 mm 110TS.

Annulus sectional area of the failed tubing was calculated as follows:

$$S = \pi\left(d^2 - D^2\right)/4, \tag{8}$$

where S is the annulus sectional area of failed tubing (mm^2); π is 3.14159; d is the inner diameter of outer casing ((184.15 − 15.83 − 15.83) mm); D is the outer diameter of failed tubing (88.9 mm).

So,

$$\begin{aligned} S &= 3.14159 \times \left((184.15 - 15.83 - 15.83)^2 - 88.9^2\right)/4 \\ &= 12{,}058\,\text{mm}^2. \end{aligned} \tag{9}$$

(iv) Pulling force due to failure of packer slip was calculated as follows:

$$\sigma_a = \left(P_{02} - P_{i0}\right) \times S/1{,}000, \tag{10}$$

where σ_a is the pulling force due to failure of the packer slip (kN); P_{02} is the external pressure of packer assuming that the packer slip failed (95.50 MPa); P_{i0} is the internal pressure of packer assuming that the packer slip failed (53.05 MPa); S is annulus sectional area of failed tubing (12,058 mm^2).

So,

$$\sigma_a = \left(95.50^2 - 53.05^2\right)\times 12{,}058/1{,}000 = 511.87\,\text{kN}. \tag{11}$$

(3) Axial load of the 105th failed tubing

It can be seen from the above data that if the packer slip failed, the axial load of the 105th failed tubing was calculated as follows:

$$\sigma_e = G + \sigma_a, \tag{12}$$

where σ_e is the axial load of the 105th failed tubing (kN); G is the string weight tension generated at a depth of 999.16 m (634.28 kN); σ_a is pulling force due to failure of packer slip (511.87 kN).

So,

$$\sigma_e = 634.28\,\text{kN} + 511.87\,\text{kN} = 1{,}146\,\text{kN}. \tag{13}$$

4.2. Collapse Test Simulating Downhole Working Conditions. Apply 1,146 kN tensile load on the same batch of tubing, and then continuously increase the external pressure, so as to conduct the external pressure collapse test under simulated working conditions. The results showed that when the external pressure reached 52.5 MPa, the tubing body failed to collapse. Table 7 shows the comparison between the simulation test results and the failure load of the 105th oil pipe of the well. The physical simulation test results of the same batch of tubing are basically consistent with the collapse failure data. It can be inferred that the packer did fail.

5. The FEA of the Tubing

In order to verify the influence of abnormal axial load on collapse behavior, the FEA model of the failed pipeline was established according to the actual outer diameter, wall thickness, and other geometric dimensions of tubing (see data in Figure 8). The axial loads under different working conditions during service were simulated and analyzed to study the stress state of failed tubing under different working conditions. The modeling of tubing was based on the actual geometric dimension measurement results of tubing, and the finite element model was established according to the axial load. The mesh of the established model is divided, as shown in Figure 9.

Apply frictionless symmetrical constraints on both ends of the tubing model, and then apply an axial load of 0–1,146.3 kN on the inner wall of the tubing to simulate

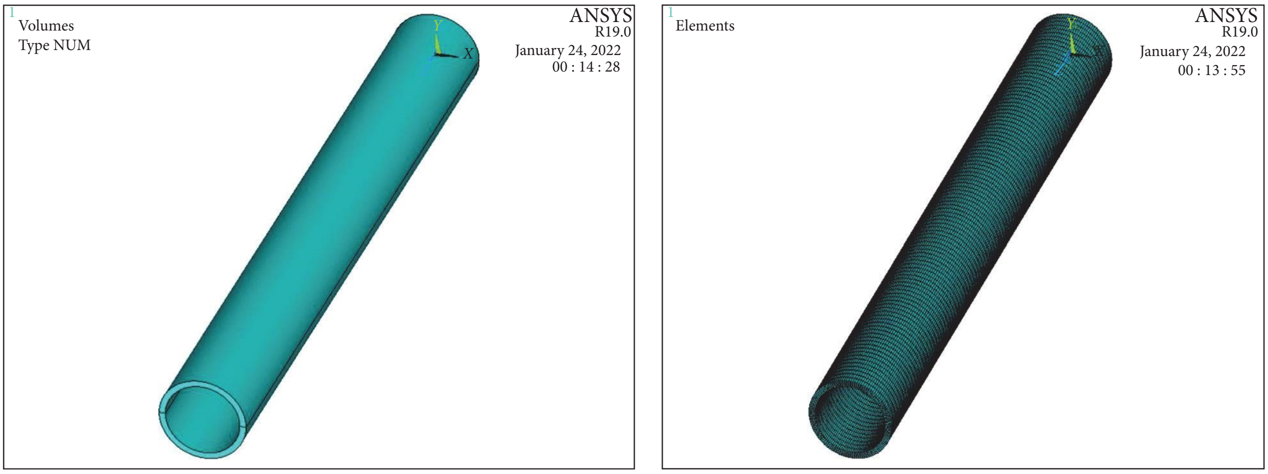

(a) (b)

FIGURE 8: Tubing FEA model (a) and the modeling of the tubing (b).

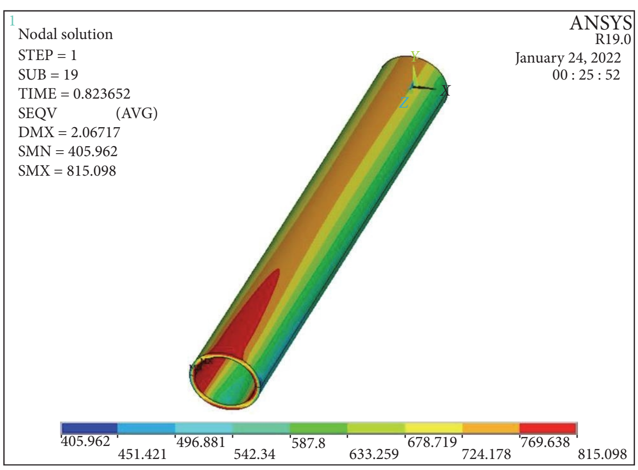

FIGURE 9: Equivalent stress distribution of axial load (Z-axis) on the same batch of tubing.

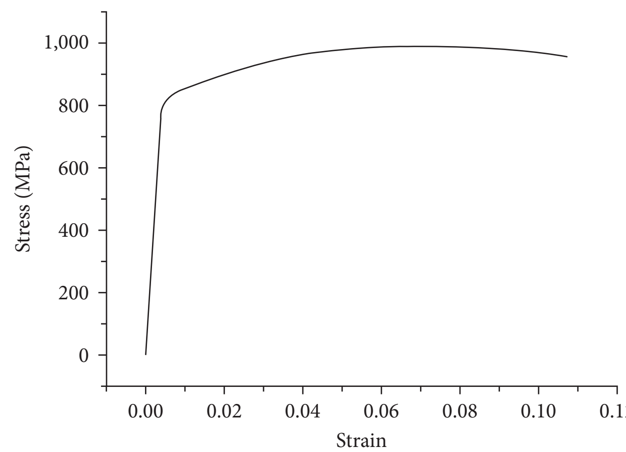

FIGURE 11: Tensile stress–strain curve of the tubing in the same batch.

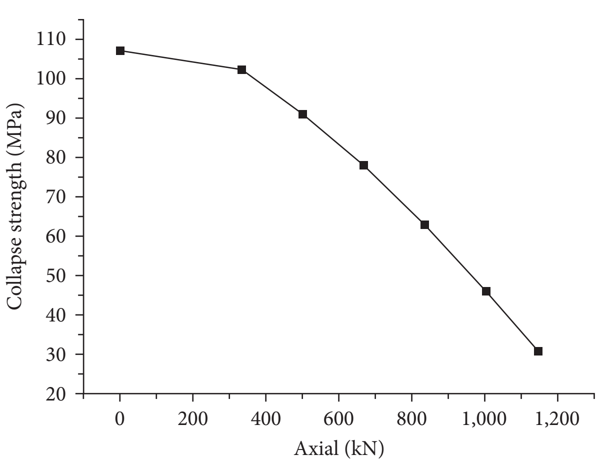

FIGURE 10: Relationship between axial load and collapse strength of tubing in the same batch.

the collapse resistance of the tubing in different axial loads., as shown in Figure 9. According to the calculation of the finite element model, if the oil pipe is subjected to an axial load of 1,146 kN in actual service, its collapse strength is 30.75 MPa. Figure 10 shows the calculation results. Therefore, if the packer slip fails in the well, it can slide freely, resulting in an axial load of 1,146 kN. When the external pressure is greater than 30.75 MPa, it will inevitably lead to collapse failure.

The analysis type of FEA was static. The nature of the solving approach adopted implicit calculation. The selected material properties were elastoplastic. The nature of the hardening approach adopted isotropic and isotropic hardening. The elastic moduli used for the simulation was 210 GPa, and Figure 11 shows the results of tensile stress–strain curve of the tubing in the same batch. The number of elements and nodes used to perform the final simulation were 127,000 and

596,000, respectively. The element types used in the model were 20 nodes and hexahedrons.

The FEA adopts 3D plane stress, assume that the upper end of the tubing is fixed and constrained, and the *X*, *Y*, and *Z* ends are constrained; the lower free end of the tubing is free of displacement, only subject to tensile load, and the cross-section is loaded with tensile load. There is an external pressure load on the outer surface of the tubing.

While in actual well conditions, the *X*, *Y*, and *Z* ends are stressed, the coupling end of the tubing is constrained, and the tubing is under the external pressure of the plane strain state.

6. Analysis and Discussion

6.1. Cause Analysis of Tubing Collapse. The outer diameter and wall thickness of the failed tubing were measured, magnetic particle inspection, physical and chemical inspection, and microstructure inspection were carried out and analyzed. The test results showed that the yield strength of the failed tubing increased due to deformation hardening. The chemical composition, Charpy impact test, and Rockwell hardness test results of the failed tubing met the requirements of ordering technical standards. There was no abnormal microstructure in the failed tubing.

The outer diameter and wall thickness of the tubing in the same batch were measured, physical and chemical inspection, collapse strength inspection were carried out and analyzed. The test results showed that the chemical composition, tensile property, Charpy impact test, and Rockwell hardness test results of this batch of tubing met the requirements of ordering technical standards.

A collapse test simulating downhole working conditions of the same batch of tubing was carried out, which reproduced the actual situation of this collapse failure in the well. Also, the local FEA of the string was carried out. From the above, It can be seen that the reason for the tubing collapse failure is that the packer lost its sealing function, resulting in abnormal pressure in the gas well annulus. Under the action of abnormal axial load and external pressure, the 105th downhole tubing collapsed.

6.2. Analysis of Packer Unsealing Factors under Special Well Conditions. In highly deviated wells, due to the large friction, it has an adverse impact on the setting of the packer and the action of downhole switching tools. The five effects (piston effect, bulging effect, friction effect, temperature effect, and spiral buckling effect) and the axial displacement caused by axial force may cause the packer to unseal. The gas well environment containing H_2S will also have an adverse impact on the performance of packer materials.

Specific reasons for the failure of the packer in the well may include the following situations:

(1) The material of the packer slip was soft. Under the action of dynamic load, its engagement with downhole casing was unstable and slipping, and then it would result in its slip failure.

(2) The outer diameter of the packer tool was too small, or the inner diameter of the tool was too large, which did not fit well with the inner wall of the casing, and then it would result in the failure of the packer.

(3) Under the condition of high temperature and high pressure and H_2S containing well, creep failure of the packer seal occurred.

(4) Under the pressure load of the well condition, the shear pin of the packer faild, and then it would result in the failure of the packer.

So, it is necessary to carry out a performance verification test of the packer simulating actual working state, so that its performance is stable in special well conditions.

7. Conclusions and Suggestions

Macroscopic observation, magnetic particle inspection, outer diameter and wall thickness measuring, physical and chemical inspection, optical microscopy, and collapse strength inspection were carried out. The comprehensive analysis, including theoretical analysis on the mechanics of collapsing tubing string and reproduction of collapse test simulating downhole load conditions, was used to analyze collapse failure accidents. Finally, the verification analysis of the collapse test is carried out by using FEA. The following conclusions can be drawn:

(1) The chemical composition, outer diameter, wall thickness, tensile properties, Charpy impact, and collapse strength test results of this batch of tubing all meet the tubing ordering technical standard requirements for this gas well.

(2) Assuming that the well packer slip was unsealed and could slide freely, the mechanical theoretical analysis of collapsing tubing string and collapsing test under simulated working condition load was carried out, which reproduced the load stress of this collapse failure and proved that the packer did fail.

(3) The reason for the tubing collapse failure is that the packer lost its sealing function, resulting in abnormal pressure in the gas well annulus. Under the action of abnormal axial load and external pressure, the 105th downhole tubing collapsed.

(4) The FEA calculation results show that the lower the yield strength of the tubing body, the lower the collapse strength of the tubing. When the external pressure is greater than 30.75 MPa, it will inevitably lead to collapse failure in case of packer is unsealed.

(5) In order to avoid the occurrence of such failure accidents, it is recommended to do some verification tests to prevent the packer from losing sealing. The verification tests include packer slip material performance, the dimensional changes of packer tool outer diameter and inner diameter, the creep behavior of the packer seal, and the performance of shear pin under actual working conditions, especially in the environment containing H_2S.

On the basis of theoretical calculation and analysis, the first simulated collapse test simulating underground working conditions is conducted in this study. Analyzing the collapse failure work and putting forward suggestions to effectively prevent similar failures from happening again are of great significance to the oilfield.

Data Availability

The authors confirm that the data supporting the findings of this study are available within the article.

Disclosure

The employer is the Tubular Goods Research Center of CNPC, which is approved to publish the article.

Conflicts of Interest

The authors declare that they have no conflicts of interest.

References

[1] Z. Zhang, Y. Zhou, J. Fu, M. Chen, W. Li, and T. Shi, "Wellbore integrity design method for sour gas wells," *Natural Gas Industry*, vol. 30, no. 3, pp. 67–69, 2010.

[2] J. C. C. Dethlefs and B. Chastain, "Assessing well integrity risk: a qualitative model," *SPE Drilling & Completion*, vol. 27, no. 2, pp. 294–302, 2012.

[3] R. Samuel, "Well integrity management system (WIMS): coupled engineering analysis," (2023-11-16)

[4] B. Singh, P. Jukes, B. Poblete, and B. Wittkower, "20 Years on lessons learned from piper alpha. The evolution of concurrent and inherently safe design," *Journal of Loss Prevention in the Process Industries*, vol. 23, no. 6, pp. 936–953, 2010.

[5] R. F. Mitchell, "New concepts for helical buckling," *SPE Drilling Engineering*, vol. 3, no. 3, pp. 303–310, 1988.

[6] R. F. Mitchell, "Comprehensive analysis of buckling with friction," *SPE Drilling & Completion*, vol. 11, no. 3, pp. 178–184, 1996.

[7] A. Lubinski, "A study of the buckling of rotary drilling strings," *API Drilling and Production Practice*, pp. 178–214, 1950.

[8] A. Shokry and A. Elgibaly, "Well design optimization through the elimination of intermediate casing string," *Journal of King Saud University - Engineering Sciences*, vol. 34, no. 8, pp. 571–581, 2022.

[9] A. I. Mohammed, B. Oyeneyin, M. Bartlett, and J. Njuguna, "Prediction of casing critical buckling during shale gas hydraulic fracturing," *Journal of Petroleum Science and Engineering*, vol. 185, Article ID 106655, 2020.

[10] J. Zhang, G. Yin, Y. Li, and L. Zhang, "Buckling configurations of tubular strings constrained in three-dimensional curved wellbores," *Journal of Petroleum Science and Engineering*, vol. 195, Article ID 107953, 2020.

[11] X. C. Tan and P. J. Digby, "Buckling of drill string under the action of gravity and axial thrust," *International Journal of Solids and Structures*, vol. 30, no. 19, pp. 2675–2691, 1993.

[12] A. I. Mohammed, B. Oyeneyin, B. Atchison, and J. Njuguna, "Casing structural integrity and failure modes in a range of well types—a review," *Journal of Natural Gas Science and Engineering*, vol. 68, Article ID 102898, 2019.

[13] Y. Liao, X. Sun, B. Sun, Z. Wang, J. Zhang, and W. Lou, "Wellhead backpressure control strategies and outflow response characteristics for gas kick during managed pressure drilling," *Journal of Natural Gas Science and Engineering*, vol. 75, Article ID 103164, 2020.

[14] Y. Qian-bei, W. Xiao-xiao, L. Yue-qiu, C. Wen, and Z. Qiang, "Failure evaluations for packers in multistage fracturing technology with immobile strings," *Journal of Petroleum Science and Engineering*, vol. 206, Article ID 109039, 2021.

[15] K. Deng, Y. Lin, H. Qiang, D. Zeng, Y. Sun, and L. Xinxin, "New high collapse model to calculate collapse strength for casing," *Engineering Failure Analysis*, vol. 58, pp. 295–306, 2015.

[16] S. R. Taheri, A. Pak, S. Shad, B. Mehrgini, and M. Razifar, "Investigation of rock salt layer creep and its effects on casing collapse," *International Journal of Mining Science and Technology*, vol. 30, no. 3, pp. 357–365, 2020.

[17] X. Guo, J. Liu, L. Dai et al., "Safety evaluation method of tubing strings in high-pressure, high-temperature and high-yield gas wells based on FIV analysis," *Engineering Failure Analysis*, vol. 120, Article ID 105044, 2021.